Eur. Phys. J. B **38**, 261–268 (2004)
DOI: 10.1140/epjb/e2004-00118-9

THE EUROPEAN PHYSICAL JOURNAL B

Networks in metapopulation dynamics

V. Vuorinen[1], M. Peltomäki[1], M. Rost[2], and M.J. Alava[1,a]

[1] Laboratory of Physics, Helsinki University of Technology, 02015 Espoo, Finland
[2] Abteilung Theoretische Biologie, IZMB, Universität Bonn, 53012 Bonn, Germany

Received 24 October 2003 / Received in final form 8 December 2003
Published online 14 May 2004 –

Abstract. The behavior of spatially inhomogeneous populations in networks of habitats provides examples of dynamical systems on random graphs with structure. A particular example is a butterfly species inhabiting the Åland archipelago. A metapopulation description of the patch occupancies is here mapped to a quenched graph, using the empirical ecology-based incidence function description as a starting point. Such graphs are shown to have interesting features that both reflect the probably "self-organized" nature of a metapopulation that can survive and the geographical details of the landscape. Simulations of the Susceptible-Infected-Susceptible model, to mimick the time-dependent population dynamics relate to the graph features: lack of a typical scale, large connectivity per vertex, and the existence of independent subgraphs. Finally, ideas related to the application and extension of scale-free graphs to metapopulations are discussed.

PACS. 87.23.Cc Population-dynamics and ecological pattern formation – 89.75.Hc Networks and genealogical trees – 89.75.Fb Structures and organization in complex systems

1 Introduction

Population dynamics or ecology offer numerous applications for stochastic processes like directed percolation and other related models studied by statistical mechanics. Their characteristics are determined by the structure of the underlying habitat or landscape. A very common class are ensembles of habitat patches, where each single patch is too small to carry a stable population but the population can survive by constantly colonizing empty patches [1]. In the biological literature such systems are called *metapopulations* [2,3]. Metapopulations appear in many different organisms, e.g., the Spotted Owl in Southern California [4] or the European nuthatch [5], the land snail *Arianta arbustorum* in northern Switzerland [6], water voles in Scotland [7] or the American pika [8], even spatial aspects of HIV in lymphoid tissue can be captured by a metapopulation model [9]. The perhaps best studied cases are insects, such as the Granville fritillary butterfly *Melitaea cinxia* on the archipelago of Åland in the Baltic Sea between Sweden and Finland (60° northern latitude, 20° eastern longitude) [10]. Its larvae feed on host plants, *Plantago lanceolata* (Plantaginaceae) and *Veronica spicata* (Scrophulariaceae) growing on well distinct meadows which form the butterfly's habitat patches. In the plants' centre the larvae form small nests around which they spin a white web, which is the easiest to recognize indicator that a habitat patch is occupied.

In modeling population dynamics certain features are isolated or highlighted and then compared with field observations. Thus one hopes to find and understand the key mechanisms behind the observed phenomena. Models exist on different levels of abstraction. The state of a population could, e.g., be rendered by an exact list of locations of each individual, or by a mere number of the total population size. In the case of the butterfly metapopulation considered here it makes sense to consider each patch of habitat as either populated or empty, thus introducing a state variable $\rho_i = 1$ or 0 for each patch i. Insects lay their eggs on host plants which are so dense in each patch that after a short while the entire patch will be colonized, typically after a few weeks. In the same way, extinction events hit the patch as a whole. On the other hand patches are sufficiently isolated by their mutual distance which is substantially larger than their respective sizes, so colonization of one patch does not immediately imply a new population on a neighbouring patch. This process is much slower and it may take years before an empty patch gets colonized. This discrete state space ($\rho_i = 1/0$) is different from the original approach of Levins [1] where population dynamics is rendered by a system of coupled ordinary differential equations (ODEs) for the population sizes in each patch.

Migration couples the population in different patches, and the coupling strength depends on their mutual distance and the geography of the landscape between the patches. Ecologists commonly use the term *incidence* for the intensity of immigrant arrival to a patch from all other

[a] e-mail: mja@fyslab.hut.fi

patches [10]. In many models the contribution of one given patch to the incidence of another one is weighted by a real number. On a very basic and abstract level the patch connection may be simplified by a *network* of patches with links between each pair of patches when substantial migration is possible and without links if it is negligibly small.

In this article we present the statistical properties of the network structure inferred from the habitat of the Granville fritillary butterfly *Melitaea cinxia*. The basic idea is to condense the original network information into a graph, using the incidence functions of metapopulations together with a threshold to establish fixed or quenched links between any pair of coupled habitats. This description holds a number of parameters, that are in essence empirical — either measurable or then related to the question what is the best effective value so as to recover other measurable properties. These graphs turn out to be interesting: they provide examples that have either *power-law* distributions for the "degree" or the number of neighbors for vertices, or possess in general for relevant parameters a large connectivity, and a rather broad distribution thereof. Moreover the structure reflects the mapping of the patch geography (sizes, locations) via the incidence functions to an abstract graph. This is a direct example, perhaps the first realistic one, of how to obtain a connection between an interaction graph and its constituents in a real, two-dimensional world [11–13].

Then we use the graphs so obtained (in Sect. 3) to study simple population dynamics, i.e. the contact process model, called susceptible-infected-susceptible (SIS) in an epidemiological context. This can be used to derive some general consequences for population dynamics on such landscapes. For scalefree graphs there have been recent developments that highlight the role of wide connectivity distributions on the survival of epidemies. In our case, these are reproduced in that the high average degree in the Åland-like graphs implies a very small effective threshold for extinction. Also, removing most-connected nodes has a relatively small effect on the average prevalence in the remaining ones. Despite this small effective threshold the butterfly species *Melitaea cinxia is* threatened by extinction on Åland, so in the model context it does have a small spreading rate compared to its local extinction rate. We also compare with the SIS-dynamics on Barabási-Albert (BA) graphs [14], to have an understanding of how the specific graph structure in the metapopulation networks affects statistical quantities being quite well understood by now in the BA-graphs (which have only weak structural correlations) [15]. Finally, we finish the paper by outlining the lessons that one learns from applying such statistical physics ideas to empirical data and related models from metapopulation dynamics.

2 Geography

The archipelago of Åland extends over an area of roughly 50 by 70 km. It consists of several thousands of islands, some of which are smaller than 100m, whereas the biggest measures about 30 km in diametre. In current field studies about 4000 patches of habitat have been identified, 1500 of which have been followed in their population status over a longer time, i.e., for more than a decade [10,16–18].

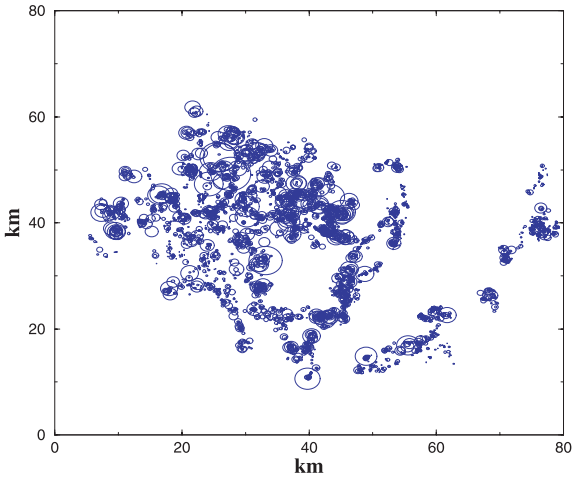

Fig. 1. The 3956 patches of habitat on the Åland archipelago, represented by circles with areas proportional to their actual sizes (between less than 10 m^2 and 10 ha) and centres at the patch locations. Regions of low and high patch density become apparent, the latter mostly on the main island. In the eastern part more distant islands form isolated groups of patches.

The habitat patches are not distributed uniformly, varying quite substantially in local density. Also their size, and with it the size of the local butterfly populations, varies over two orders of magnitude. Figure 1 shows the measured data, on the basis of which we create the graphs. One can distinguish several candidate subgraphs, based on the geometrical distances of the patches. Notice also the size distribution of the patches themselves.

Figure 2 shows the area distribution of the patches. It is evident that this has a broad character, and a rough fit to the data indicates a power law decay $P \sim A^{-2}$. An analysis of inter-patch distances reveals the high nonuniformity in the locations of patches. Figure 3 shows a histogram $h(r)$ of distances r between each pair of patches in bins of width 800 m. These data, as well as those for $P(A)$ are in practice constructed by field observations, by using GPS-receivers to construct distance- and size-data sets with a usual GPS accuracy level (∼10 m). The midpoints of each patch, from which the distances are computed, are roughly set at the respective centers of gravity.

There is a remarkably high number of close pairs, we find $\lim_{r\to 0} h(r) = h_0 > 0$ which is significantly different from the form $h(r) \simeq 2\pi\ \nu\ r$ belonging to patches distributed according to a two-dimensional Poisson process with uniform density ν. In Figure 1 one can find such regions of very high patch accumulation, e.g., in the area north of the big bay in the centre of Åland.

Different habitat patches are coupled with each other by dispersal, immigration and finally colonization of empty patches starting from inhabited locations. In many theoretical approaches for the sake of simplicity dispersal is assumed to be uniform in the landscape and not

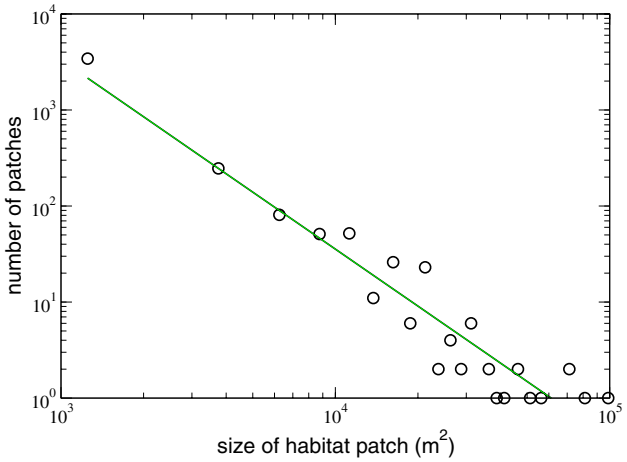

Fig. 2. Number of patches as a function of patch sizes on double logarithmic scale. The line is meant as a guide to the eye, and indicates a $1/A^2$-behavior.

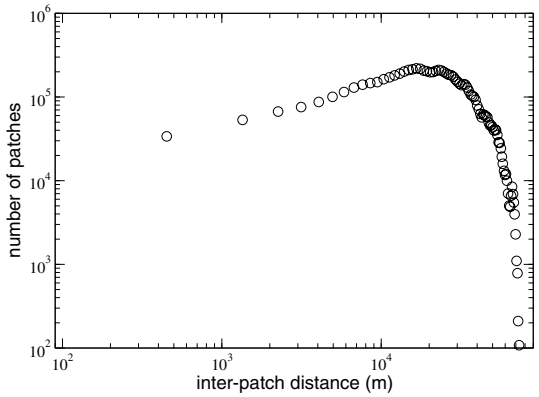

Fig. 3. Histogram $h(r)$ of pairwise patch distances r taken in bins of width 800 m. High accumulation lets $h(r \to 0)$ approach a *finite* value. Note equation (1), and the role of r therein.

to depend on special geographic features such as rocks, vegetation profile, water, or others. A central concept in describing the dynamics is the *incidence function* or incidence at a patch, representing the immigration intensity to that given patch [2,10,18]. The colonization probability of an empty patch subject to immigration for some period of time is an increasing function of the incidence. Patches which are close and well connected to many others therefore have a higher colonization rate than more isolated ones. The importance of inter-patch connectivity makes it an obvious choice to try to represent the landscape of habitat patches by a graph of linked nodes.

3 Graph formation

The main idea in mapping the metapopulation dynamics onto a graph is to consider the possible intensity of immigrants to patch i due to emigrants form patch j. Here it is helpful to define a *migration kernel*

$$f_{ij} = C A_i^{\beta} A_j^{\beta'} \exp\left(-r_{ij}/D\right), \qquad (1)$$

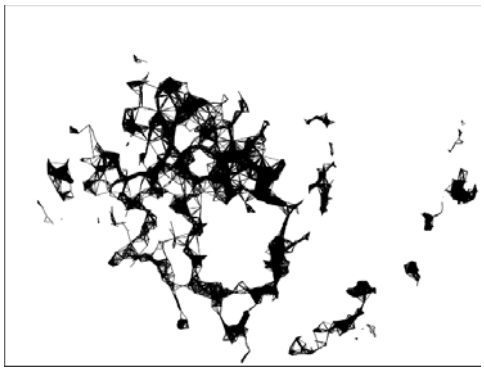

Fig. 4. Example of a network connecting the patches shown in Figure 2, obtained with parameter set PL (see text). Immediately visible are (i) a high degree of connectivity and (ii) several (semi)independent subgraphs corresponding to different larger and more distant islands in the archipelago.

where C is a constant prefactor, the A_i's are the patch sizes, β and β' exponents relating the migration of a population to/from a patch to its size, and D takes into account the proper normalization of the dispersal length. The migration kernel decays with increasing inter patch distance $r_{ij} = |\mathbf{x}_i - \mathbf{x_j}|$.

The exponential decay accounts for the loss of butterflies when crossing unsuitable terrain (so called *matrix* between habitat patches). Typical dispersal lengths are between 100 m and 1 km [2,10,16,17,19]. Larger patches supply more emigrants and in turn attract more immigrants, but this effect is not arbitrarily strong, so a reasonable range is $0 < \beta, \beta' \leq 1$. This last choice is not restricted to the models of *Melitaea cinxia* on Åland but applies to any metapopulation system with varying patch sizes.

Out of the set of patches i we form a graph so that two patches j, k are connected with a fixed directed link (or edge), if the condition

$$f_{jk} > T \qquad (2)$$

is fulfilled, with T being a free parameter. In the case $\beta = \beta'$ considered in the simulations presented here, all $f_{jk} \equiv f_{kj}$, and the resulting graph is symmetric.

Such a threshold is biologically reasonable, accounting for the observation that empty patches become colonized only if a certain amount of immigrants is present. A butterfly will be more likely to approach a patch if possible mating partners are available, moreover the presence of other individuals acts as an indicator for resource quality in the patch to be populated [2].

Note that the kernel f_{ij} in (1) only depends on the two patches i and j. For simplicity the effect of other patches distracting migrants is neglected, but one could envision a "fully nonlocal" model of inter patch migration [21]. Figure 4 shows an example of an ensuing network, for the parameter set that produces power-law-like connectivity distributions (see below), making it evident that such networks are highly connected.

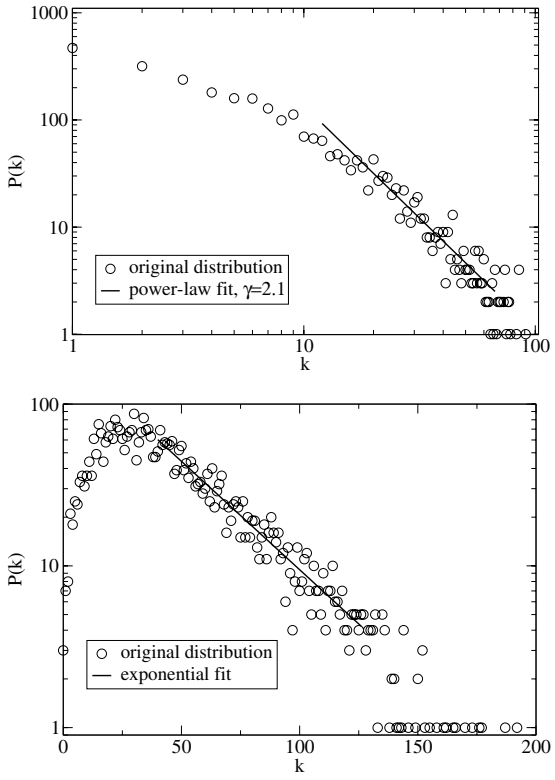

Fig. 5. Example degree distributions, i.e., the number $P(k)$ of nodes with k neighbours, obtained from networks with parameter sets PL (upper graph) and EXP (lower graph) respectively (see text) resulting in power-law and exponential decay of $P(k)$.

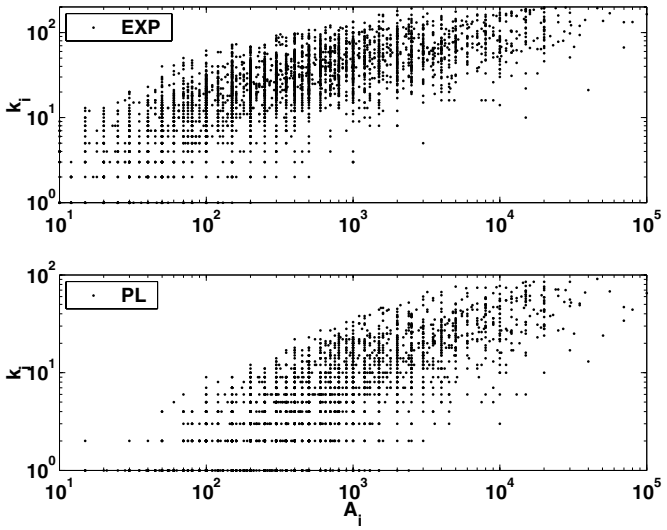

Fig. 6. A scatter plot indicating correlations between patch sizes A_i and connectivities k_i, inferred by construction of the graph.

Further information can be obtained by considering the degree distributions $P(k)$, i.e., the number of nodes with k links pointing to neighbours. These are very broad – but by tuning the parameters, in particular $I \equiv T/C$ and β, the approximate shape of $P(k)$ can be changed. We obtain in the case of Figure 5 two different forms one of which resembles a *power-law*, with a scaling $P \sim k^{-2.1}$, and another one which resembles an *exponential* distribution but with a decay parameter that implies a slow decay. The parameters used were $D = 500$, $\beta = \beta' = 1.0$ and $I \equiv T/C = 2 \times 10^5$ for the power law (PL) case and $D = 1000$, $\beta = \beta' = 0.25$ and $I \equiv T/C = 3$ for the exponential (EXP) distribution of connectivities. One peculiarity of the EXP-network are the smaller $P(k)$ for small k: Due to the relatively large dispersal length D very few nodes remain completely isolated. We have for the average degree that $\langle k \rangle$ is about 7.7 and 44.9, for the PL and EXP cases respectively.

By the construction of the graph via the migration kernels f_{jk} the connectivity k_i of a patch i gets correlated with its size A_i as is shown in Figure 6.

The graphs consist of *isolated subgraphs* for ecologically sensible parameter ranges, which roughly correspond to larger islands in the group (e.g. Föglö and Kumlinge in the eastern part). This will be shown to be reflected in the behavior of models defined on such graphs. We do not study in detail the number and size distribution of the separate components; in the cases considered below there is typically "a few", up to maybe ten such present.

One should also note the presence of correlations in the structure. The underlying geographical graph construction induces correlations between degrees of neighbouring nodes: Neighbours of highly linked nodes tend to have many neighbours themselves, because typically they lie in regions of high patch density. Figure 7 shows these correlations for the parameter set EXP (a PL graph would have qualitatively the same results), in its upper panel the number $P(k, k')$ of links connecting pairs with degrees k and k' normalised by the number one would expect in an uncorrelated graph, $k\ k'\ P(k, k')$. Generally the degrees of neighbouring nodes tend to be similar, and this behaviour becomes more prominent for larger k. The lower panel contains the average degree of neighbouring nodes $\langle k_{\rm nn} \rangle$ of nodes of degree k, the raw data are represented by empty circles the solid line is obtained by convolution with a smooth kernel. Thus the behavior of the butterfly metapopulation resembles social networks, there is *assortative* mixing [22]. Notice also that the scaling of Figure 7 is almost like a power-law, with an exponent close to 0.5. This type of scaling has in mean-field-like models strong implications on clustering [20]. Here, it turns out to be so that in analogy with the implications of $\langle k_{\rm nn} \rangle$ the average probability for two nearest neighbors to be connected with a link is substantial ($\sim 0.6 \ldots 0.7$), and the $C(k)$-distribution of clustering of nodes with a degree k is broad, and decaying with k.

4 The SIS model

The contact process or the SIS model is a simple description of the spreading and dynamics of epidemics. The strong seasons in northern latitudes impose an annual life cycle on the population of *Melitaea cinxia*, so all patch

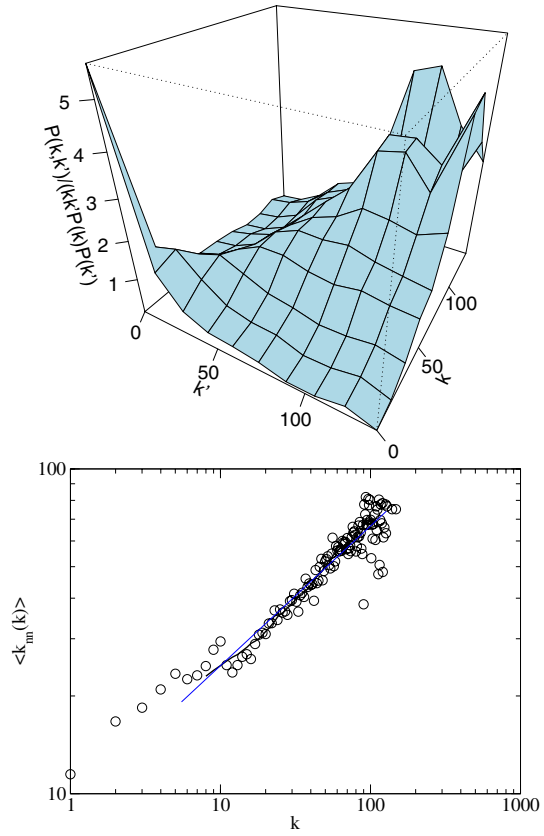

Fig. 7. Correlation in the degree of neighbouring nodes for the parameter set EXP (a PL gives no qualitative difference). Upper panel: $P(k,k')$, number of connected pairs between nodes of degrees k and k' normalised by its expectation in an uncorrelated graph, $k\,k'\,P(k,k')$. Lower panel: $\langle k_{\rm nn}\rangle(k)$, average degree of neighbours of a nodes as a function of its own degree (circles) with smoothing of the data over a window of width 15 (solid line). A rough fit indicates $\langle k_{\rm nn}\rangle \sim k^{1/2}$.

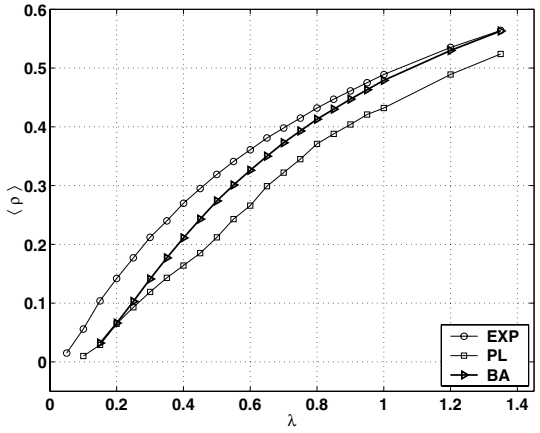

Fig. 8. Average activity $\rho(\lambda)$ vs. spreading rate λ for parameter sets PL and EXP, compared to a Barabási-Albert graph of the same size.

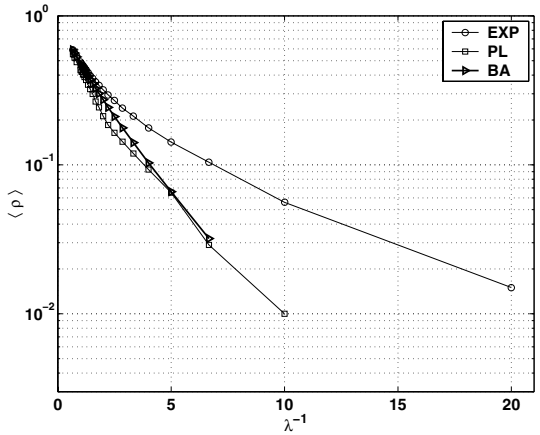

Fig. 9. Same data as in Figure 8 plotted in logarithmic scale over $1/\lambda$. Straight lines indicate $\langle\rho\rangle \sim \exp(-\text{const.}/\lambda)$, which is not quite obeyed by the data from the Åland network in contrast to the BA graph which comes closer to this behaviour [15].

occupancies are updated in parallel once per year. Nevertheless characteristic features of its dynamics can be captured by the conceptually simpler continuous time processes.

In order to adapt the time scales recall that typical single patch populations last for only a couple of years [2,10]. In continuous time it is therefore sensible to set a death rate of 1 per year as a frame of reference to which all other rates and times have to compare. As populated nodes on the graph become empty at rate 1, empty patches become colonized with rate λ (given as a model parameter) if at least one neighbour patch is populated. The influence of graph structure has recently been highlighted in the context of scale-free networks, for which $\langle k^2\rangle$ may diverge in the limit of large node numbers (for a broad $P(k)$, e.g., for power-laws $\sim k^{-3}$, like the Barabási-Albert model). The practical outcome is a vanishing critical spreading rate $\lambda_{\rm c}$ in the limit of infinite network sizes, i.e., there are always parts of the network with high enough connectivity to sustain a population no matter how small the spreading rate λ.

We investigated the behaviour of the SIS model in the Åland graphs by Monte Carlo simulations and compare them to Barabási-Albert networks [14] with $m=3$ of the same size (3956 nodes). The main features are depicted for two kinds of sample networks in Figures 8 and 9, both for a case of a power-law decay in $P(k)$ (parameter set PL) and exponential decay (parameters EXP).

The conclusion is easy: for such large connectivities the effective threshold is *small*. Moreover the influence of the actual form of the degree distribution is quite negligible, the Åland graphs nevertheless differ slightly from BA networks in the functional form of $\rho(\lambda)$. The latter exhibit a clear behaviour $\rho \sim \exp(-\text{const}/\lambda)$ in analogy with mean-field behaviour of the SIS model on scalefree networks [15], as is visible in Figure 9. The data from the Åland networks seem to follow rather a functional form $\exp(-\text{const}/\lambda^\gamma)$ with some effective $\gamma > 1$, resulting in a bending line in Figure 9, though the PL data is close to the MF-scaling. This may be due to the presence of highly linked subgraphs of different sizes, each of which behaves mean-field like, such that the bending line could be a sum

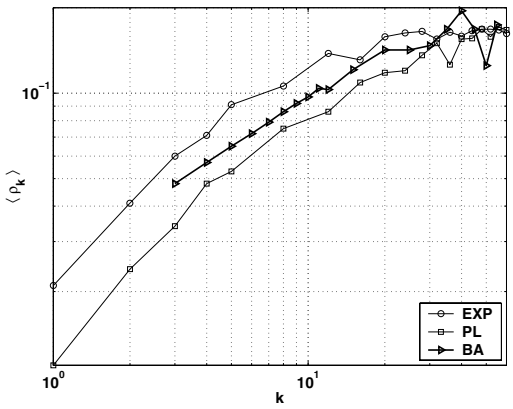

Fig. 10. Comparison of $\rho(k)$ as a function of k between a BA-graph ($N = 3956$, $m = 3$) and the Åland graphs for parameter sets PL and EXP.

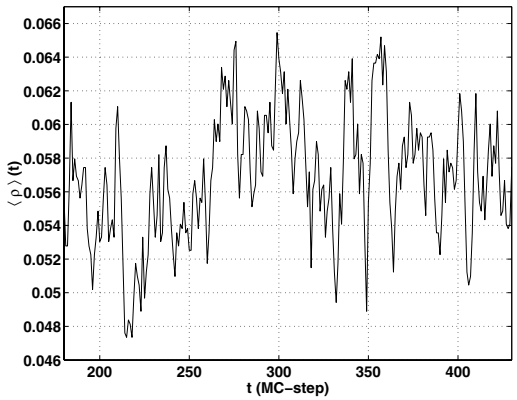

Fig. 11. A time series of the average activity $\langle \rho \rangle$ in an graph with parameters EXP exhibits large fluctuations for $\lambda = 0.2$, which is well above λ_c (average activity $\langle \rho \rangle = 0.056$).

of several straight lines with different slope each. Note that there is evidence that in the presence of clustering the survivability of an epidemic is enhanced, since, simply put, the infection process has more routes available between any pair of empty and occupied nodes [23].

More microscopic studies of the role of the degree are depicted in Figure 10. Here we consider $\langle \rho_k \rangle$, the average activity of nodes with degree k. It is distinctly different from that of a Barabási-Albert graph with the same average activity, prevalence (we tuned λ to achieve this) and same size N. On all Åland networks (PL and EXP) the average activity of nodes with degree k increases with k sublinearly, until saturation takes place, $\langle \rho_k \rangle \equiv \langle \bar{\rho} \rangle$. Meanwhile the BA-case exhibits again the well-known scaling, which is close to linear according to the MF-solution [15].

While otherwise the epidemics is strongly mean-field like, one should however note that there are both interesting fluctuations and correlations. The time series of the spatially averaged population size, related to $\bar{\rho}(t)$, exhibits large fluctuations even when λ is not too close to the extinction threshold λ_c, as shown in Figure 11 for an average activity $\langle \rho \rangle = 0.056$. The fluctuations are significantly larger than one would expect for an uncorrelated process, $\Delta\rho_{\mathrm{uncorr}} \simeq \sqrt{\langle \rho \rangle / N} \simeq 0.004$. The larger fluctuations are caused by strong correlation within highly linked subnetworks which get colonized or go extinct all at once. These turned out to be quite important in the ecological description of the population dynamics to ensure conservation of the species *Melitaea cinxia* and were classified as *semi-independent networks* (SIN) [18]. The system is relatively robust against removal of single nodes, as long as the highly linked subnetworks remain functioning. We have checked this in several ways, e.g., by deleting highly linked nodes from the graph. A qualitative interpretation is that within the subnetworks there remains always a "way around" the removed nodes — unless too much habitat has been taken out.

The influence of subgraphs becomes visible also in the temporal autocorrelation of the activity, which is represented in Figure 12 for the average activity as well as for

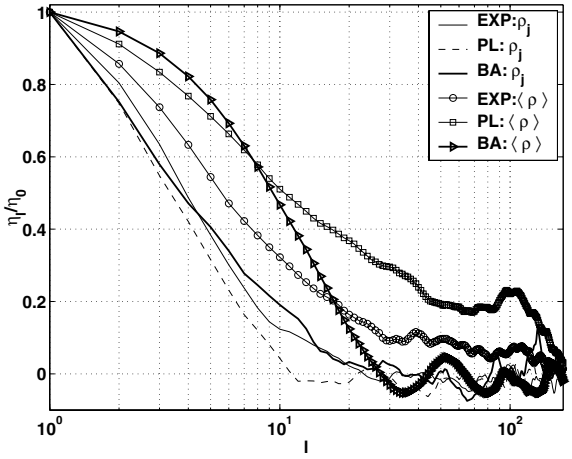

Fig. 12. Temporal autocorrelation of the spatially averaged activity and at randomly chosen patches with intermediate link degree ($k = 30$). For detailed definition of η_l see text.

randomly chosen nodes. Here the autocorrelation of the average activity $\bar{\rho}$ in the system over a time lag of l steps is defined

$$\eta_l = \langle \bar{\rho}(t)\bar{\rho}(t+l) \rangle - \langle \bar{\rho}(t) \rangle \, \langle \bar{\rho}(t+l) \rangle. \qquad (3)$$

Autocorrelations of single nodes (here an example of a node i with coordination number $k = 30$ is taken) are defined analogously, but with $\rho_i(t)$ instead of $\bar{\rho}(t)$. The autocorrelation times in the Åland networks (PA and EXP) turn out to be quite short, which indicates a relatively fast equilibration within highly linked subclusters [23]. The averaged η-plots show again a definite difference between the BA-model and both Åland cases. In particular the PL set exhibits slowly decaying correlations. Notice that the average connectivity is much smaller than for the EXP one, and close to the one of the BA graphs. It would be interesting to try to locate such correlations to any particular subgraph.

Likewise, one can consider the relation of $\langle \rho_i \rangle$ vs. A_i. For large spreading rates (e.g., $\lambda = 1.5$) essentially all nodes are active with probability $\lambda/(1+\lambda) = 0.6$. As λ decreases, clusters of lower activity, e.g. with $\langle \rho_i \rangle \simeq 0.12$

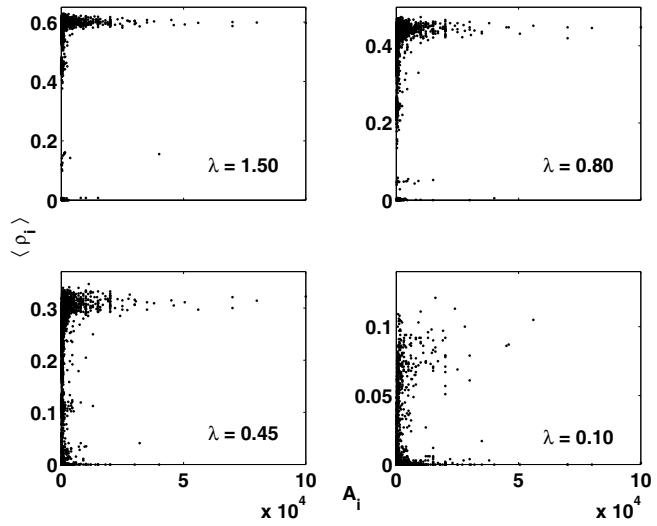

Fig. 13. Scatterplot of the average activity of each node versus its patch size for various spreading rates λ in a network for parameter set PL. For large $\lambda = 1.5$ virtually all plots have the same (average) activity, for small $\lambda = 0.1$ most patches are empty. Subgraphs with lower average activity are visible, in particular at intermediate values of λ.

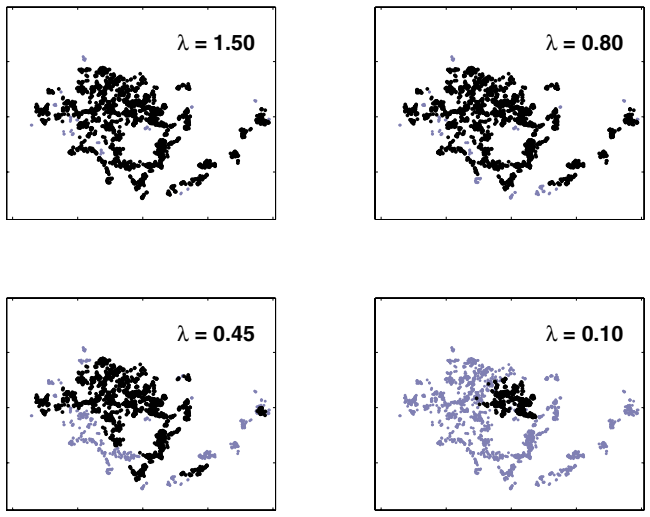

Fig. 14. Same data as Figure 13, but represented in geographical space. Fat black dots: patches are alive ($\langle\rho_i\rangle > 0.01$) or practically extinct (fat grey dots, $\langle\rho_i\rangle < 0.01$.)

at $\lambda = 0.45$ become visible, which correspond to medium sized and effectively isolated subgraphs. They also have a higher critical spreading rate $\lambda_c^{\text{subgraph}}$ below which they lose their populations. At low $\lambda = 0.1$ most parts of the network have become empty and many points in the plot are found at the axis $\langle\rho_i\rangle = 0$, in particular the four largest patches which have remained populated at average population density for higher values of λ.

5 Conclusions

The behavior of populations in metapopulation landscapes provides an interesting example of a system that can be discussed in the form of dynamical models on graphs. These have properties quite unlike those of idealized models: there are correlations that carry over from the underlying geography, and the connectivity is very high. In the simulations of the SIS model on such graphs one discovers that the main relevant feature is the very large average degree $\langle k\rangle$. Consequently the effective critical value of the SIS spreading parameter λ is small. Likewise, for reasonable parameters the graph is essentially broken into several independent subgraphs, or semi-independent networks in the ecologists' terms.

From a biological viewpoint an attempt to map metapopulation dynamics into the contact process on a quenched graph is a strong simplification. It is of course more intuitive to principally allow for migration between any pair of patches j and k and to give the links some real connection numbers $0 < c_{jk} \leq 1$ which, e.g., could be chosen proportional to the f_{jk} in equation (1). Empty patches become colonized by sufficiently large number of immigrants, which in such a model can be supplied from *several different* patches, whereas our simplified graph model considers only colonization from one patch to another. This kind of construction is at the heart of the incidence function model [10]. Multi-patch immigration is however contained here intrinsically, by a higher colonization rate in higher linked patches, which rarely find themselves without any populated neighbour.

Despite its simplicity the model reproduces several features observed in the real population and by some more realistic models: The cooperative population of many patches, the tendency to have independent subpopulations on highly linked subnetworks which become active or inactive at once in a correlated manner. This enhances the effect of demographic stochasticity by reducing the effective metapopulation size. The population consists of larger, but less units. Fluctuations may drive the population to extinction even if the spreading rate λ is somewhat larger than the critical λ_c, which has been observed on quite a few of the subnetworks in Åland over the last years [17]: *Melitaea* has gone extinct on some subnetworks after a series of three quite dry summers unfavourable for its host plants. In this respect it is interesting to note the slightly non-Markovian dynamics of the order parameter (Fig. 11). This is dependent on the particular choice of an incidence function, which results in the degree distribution and correlations exhibited by the final graph, and highlights the crucial role of the (empirical) parameters therein.

The autocorrelation time is more than one order of magnitude larger than the timescales involved in the elementary processes of colonization and extinction, and it is larger than on a BA-graph. Here the lifetimes of entire highly linked subgraphs of SINs become visible covering the traces of single patch dynamics. Note that the autocorrelation of single patches in a subnetwork which remains active during the measurement (lines without symbols in Fig. 12) decays faster. We conclude that these subgraphs of SINs are the important units for species' conservation issues.

For future investigations one can envision several directions. Among others, metapopulation dynamics gives rise to examples of interaction graphs that are rather unique, and are reflected in the dynamical properties of models on such graphs. An example met above is existence of correlations in $\rho(t)$ unlike in the reference model used (BA graphs). Obviously, the survival properties of finite systems become interesting in this limit.

We thank Ilkka Hanski for sharing his detailed knowledge and insight on metapopulation ecology with us in numerous discussions, as well as for providing us with the data on patch locations and sizes. This work was supported by the Academy of Finland, Center of Excellence program, and Deutsche Forschungsgemeinschaft via SFB 611 (*Skalierung in mathematischen Modellen*, MR). MR thanks Helsinki University of Technology for kind hospitality.

References

1. R. Levins, Bull. Entomol. Soc. Am. **15**, 237 (1969)
2. I. Hanski, Nature **396**, 41 (1997)
3. *Metapopulation Biology,* edited by I. Hanski, M.E. Gilpin (Academic Press, San Diego, 1997)
4. W.S. Lahaye, R.J. Gutierrez, H. Resit Akcakaya, J. Animal Ecology **63**, 775 (1994)
5. J.F. ter Braak, I. Hanski, J. Verboom, in *Modelling Spatiotemporal Dynamics in Ecology*, edited by J. Bascompte, R.V. Solé (Springer, New York, 1998), pp. 167–188
6. H. Resit Akcakaya, B. Baur, Oecologia **105**, 475 (1996)
7. W. Stewart, J.F. Dallas, S.B. Piertney, F. Marshall, S. Telfer, A. Sharul, X. Lambin, Biol. J. Linn. Soc. **68**, 159 (1999)
8. A. Moilanen, A.T. Smith, I. Hanski, Am. Nat. **152**, 530 (1998)
9. S.D.W. Frost, M.-J. Dumaurier, S. Wain-Hobson, A.J. Leigh Brown, Proc. Nat. Acad. Sci. USA **98**, 6875 (2001)
10. I. Hanski, J. Anim. Ecol. **63**, 151 (1994)
11. D. ben-Avraham, A.F. Rozenfeld, R. Cohen, Sh. Havlin, Physica A **330**, 107 (2003)
12. C.P. Warren, L.M. Sander, I.M. Sokolov, Phys. Rev. E **66**, 056105 (2002)
13. M. Barthelemy, Europhys. Lett. **63**, 915 (2003)
14. A.L. Barabási, R. Albert, H. Jeong, Physica A **272**, 173 (1999)
15. R. Pastor-Satorras, A. Vespignani, Phys. Rev. Lett. **86**, 3200 (2001); R. Pastor-Satorras, A. Vespignani, Phys. Rev. E **63**, 066117 (2001)
16. I. Hanski, M. Kuussaari, M. Nieminen, Ecology **75**, 747 (1994)
17. I. Hanski, J. Alho, A. Moilanen, Ecology **81**, 239 (2000)
18. O. Ovaskainen, I. Hanski, Theoretical Population Biology **60**, 281 (2001)
19. M. Kuussaari, M. Nieminen, I. Hanski, J. Animal Ecology **65**, 791 (1996)
20. G. Szabo, M. Alava, J. Kertesz, Phys. Rev. E **67**, 056102 (2002)
21. I. Hanski, O. Ovaskainen, Theoretical Population Biology **64**, 119 (2003)
22. M.E.J. Newman, J. Park, Phys. Rev. E **68**, 036122 (2003)
23. M.E.J. Newman, Phys. Rev. E **68**, 026121 (2003)